Photochemical & Photobiological Sciences

Accepted Manuscript

This is an *Accepted Manuscript*, which has been through the Royal Society of Chemistry peer review process and has been accepted for publication.

Accepted Manuscripts are published online shortly after acceptance, before technical editing, formatting and proof reading. Using this free service, authors can make their results available to the community, in citable form, before we publish the edited article. We will replace this *Accepted Manuscript* with the edited and formatted *Advance Article* as soon as it is available.

You can find more information about *Accepted Manuscripts* in the Information for Authors.

Please note that technical editing may introduce minor changes to the text and/or graphics, which may alter content. The journal's standard Terms & Conditions and the Ethical guidelines still apply. In no event shall the Royal Society of Chemistry be held responsible for any errors or omissions in this *Accepted Manuscript* or any consequences arising from the use of any information it contains.

ROYAL SOCIETY OF CHEMISTRY

www.rsc.org/pps

Comparison of UVA-induced ROS and sunscreen nanoparticle-generated ROS in human immune cells

Cenchao Shen[a], Terence W. Turney[b], Terrence J. Piva[a], Bryce N. Feltis[a,b] and Paul F.A. Wright[a*]

[a]School of Medical Sciences, and NanoSafe Australia, RMIT University, Bundoora VIC 3083, Australia, [b]Department of Materials Engineering, Monash University, Clayton VIC 3800, Australia

ABSTRACT

Oxidative damage to cells and tissues from free radicals induced by ultraviolet (UV) irradiation can be attenuated by sunscreen components, such as ZnO and TiO_2 nanoparticles (NPs). Although it is known that reactive oxygen species (ROS) are generated by cells upon exposure to ZnO and TiO_2 NPs, it is unknown to what extent the amount generated is altered with UV co-exposure. As it is a critical component for determining the relative risk of these NPs when used in sunscreen formulations, we have investigated ROS generation by these NPs in human THP-1 monocyte immune cells following UVA co-exposure. Whilst the applied UVA dose (6.7 J/cm^2) did not alter cell viability after 24 h, it induced significant ROS production – causing a 7-fold increase in intracellular peroxide and 3.3-fold increase in mitochondrial superoxide levels after 1 h. However, co-exposure to NPs and UVA generated the same or less

*Corresponding author.
E-mail address: paul.wright@rmit.edu.au

ROS than with UVA exposure alone, with the exception of anatase TiO_2, which showed significantly increased levels. These findings indicate that ROS generation from nanosunscreens is, in most cases, an insignificant contributor to the overall risk associated with oxidative stress from UVA exposure itself.

Keywords: nanoparticles, sunscreen, ROS, UV

1. Introduction

UV-induced reactive oxygen species (ROS) have been implicated in photocarcinogenesis and skin ageing.[1] This is because UV-induced ROS can induce DNA damage that, if unrepaired, can lead to carcinogenesis.[2] Such DNA damage includes single- and/or double-strand DNA breaks, base modifications (e.g. formation of 8-hydroxydeoxyguanosine (8-OHdG) and other oxidative products) and DNA cross-links.[2] Sunscreens contain UV attenuators, such as organic chemical and/or physical UV filters, which can prevent all forms of damage from UV irradiation. However, it has been reported that organic sunscreen UV filters can actually enhance UV-induced ROS once they penetrate the epidermis.[3]

In recent years, the effective broad-spectrum UV attenuation properties of ZnO and TiO_2 nanoparticles (NPs) have made them attractive as active components in sunscreens and other personal care products. While organic sunscreens generally absorb UV light more effectively in the UVB range, only a few are able to absorb UVA. The broadest UVA attenuation is achieved with avobenzone, but this compound tends to break down on exposure to UV light and also has potential to be photo-allergenic.[4] In contrast, ZnO possesses stable broad-spectrum UV filtering capabilities and is an attractive alternative to the less photo-stable avobenzone. Compared to chemical sunscreens, physical sunscreens do not break down under UV light and are therefore potentially longer-acting. In addition, the transparent properties of NP sunscreens make these products more aesthetically pleasing, after skin

application, than formulations containing larger, light-scattering, inorganic particles, which appear visually opaque.

As the use of NP compounds in sunscreens increases, so has public concern about their safety. One of the primary concerns raised about NPs is their potential to generate ROS, particularly when exposed to UV light.[5–7] It is important to note that similar NPs are also well-known photocatalysts used in industry, which can produce a variety of ROS for an extended period under certain conditions.[8] Furthermore, the high surface area properties of NPs can also increase the rate of generation of ROS. This was confirmed by Xia *et al.*, who reported that both mouse immune cell lines and human lung epithelial cells displayed elevated levels of mitochondrial superoxide following *in vitro* exposure to ZnO NPs.[9–10] In Braydich-Stolle's study[11], cytotoxicity profiling of TiO_2 NPs in a mouse keratinocyte cell line showed that rutile TiO_2 NPs initiated apoptosis through formation of ROS. Although there are numerous studies investigating ROS production by ZnO and TiO_2 NPs[9–14], there is currently a paucity of studies that investigate cellular ROS generation in the presence of both sunscreen NPs and UV irradiation[15,16]. As these materials are used in sunscreens, UV co-exposure is certain, and thus it is vital to investigate ROS generation in cells co-exposed to both NPs and UV, rather than solely investigate ROS generation from NP exposure alone.

It is important to consider the most appropriate form of UV irradiation for potential interactions with NP exposure in the biological test system. While UVC is

generated during industrial processes, such as in arc welding and microbial photosterilization, it is usually not biologically relevant in environmental exposure because UVC from sunlight is blocked almost entirely by the ozone layer. Both the UVA and some UVB wavelengths in sunlight reach the surface of the earth to cause biological effects. The higher energy of UVB causes more overall direct cellular damage than UVA. However, the shorter UVB wavelengths only penetrate into the epidermis, whereas UVA can penetrate through to the dermis and interact with cells of the immune system.[17]

There is negligible dermal penetration of intact metal oxide NPs past the outermost dead cell layer of the strata corneum.[18] However, any intact particles that do penetrate the skin are most likely to be scavenged by phagocytic immune cells present in the dermis and peripheral vasculature, such as macrophages and their monocytic precursors. Consequently, there is a potential for these cell types to be exposed to a higher intracellular concentration of sunscreen NPs with concurrent UVA exposure. Therefore, in this study we have co-exposed human THP-1 monocyte-like cells to both UVA and metal oxide NPs and assessed ROS generation, specifically intracellular peroxide and mitochondrial superoxide levels. We examined ROS generation in monocytes rather than macrophages because although both cell types phagocytose NPs, the lower basal ROS activity in monocytes[19,20] facilitated the direct comparison of the individual effects of UVA and NP exposure on ROS generation with the effects of UVA and NP co-exposure. We also assessed the time course of intracellular ROS

generation under these exposure conditions in order to evaluate the relative contribution and impact of UVA-induced ROS compared with sunscreen NP-generated ROS.

2. Materials and methods

2.1. Materials

ZnO NPs with primary particle diameters of 30 and 200 nm, with and without surfactant dispersant (Orotan 731 DP) were supplied by Micronisers Pty. Ltd. (Melbourne, Australia). Full physical characterization of these nanomaterials, as well as $ZnCl_2$ in culture media, have previously been reported by us.[19–22] Anatase TiO_2 (25 nm) and rutile TiO_2 (34 nm) NPs were purchased from commercial suppliers (CSIRO, Clayton, Australia).

2.2. Cell culture, UV irradiation and cytotoxicity assays.

The human acute monocytic leukaemia cell line (THP-1) (kindly provided by Department of Medicine, University of Melbourne, Melbourne, Australia) was cultured in RPMI-1640 media containing 10% fetal bovine serum (FBS), 100 mg/L gentamycin, 4.5 g/L glucose, 1 mM pyruvate, 0.05 mM 2-mercaptoethanol and 2 mM L-glutamine. Cells were cultured in a humidified incubator at 37°C and 5% CO_2. The cells were removed from their flasks and centrifuged (400 *g* for 5 min) before being resuspended in fresh media prior to being added at 10^5 cells per well in a 96-well

plate. NPs suspended in tissue culture media were added at a final concentration of 1–100 μg/mL. Immediately following the addition of NPs, the cells were exposed to a single acute dose of 6.7 J cm^{-2} UVA over 15 min in a BioSun System (Vilber Lourmat, Marne-La Vallee, France) comprising an irradiation chamber equipped with 365 nm illumination lamps, a sensor/dosimeter, calibrator, and software. Control groups included wells containing cells without NPs, and with either UVA irradiation or no UV (sham) radiation exposure – the sham irradiation group controlled for potential effects of time spent outside of the incubator during the irradiation procedure. Following UVA irradiation, the cells were returned to the incubator. After 20 h, MTS (3-(4,5-dimethylthiazol-2-yl)-5-(3-carboxymethoxyphenyl)-2-(4-sulfo phenyl)-2H-tetrazolium, CellTiter 96® aqueous kit, Promega, Madison, WI, USA) was added to each well and incubated for 4 h before being measured at 490 nm on a plate reader (FlexStation 3 Microplate Reader, Waltham, CA, USA). Wells containing only the concentration range of NPs and MTS reagent were used to control for any direct optical density effects of NPs by subtracting these values from the experimental readings. All treatments were performed in triplicate for each experiment.

2.3. Peroxide generation.

Peroxide generation was measured by 2',7'-Dichlorofluorescin diacetate (DCFDA) (Sigma, St Louis, MO, USA). Cells were centrifuged and resuspended in fresh media at a concentration of 10^6 cells/mL. Cells were then washed in phosphate-buffered

saline (PBS), followed by the addition of 100 μM DCFDA and then incubated for 30 minutes in a dark and humidified incubator at 37°C and 5% CO_2 to allow for uptake. Cells were washed again with PBS to remove extracellular DCFDA, after which fresh media was added. Cells were then seeded in black 96-well plates at 10^5 cells per well. NPs suspended in tissue culture media were added for a final concentration of 10–100 μg/mL. Subsequently, cells with NPs were co-exposed with UVA (6.7 J/cm^2). After incubation time points of 1, 4, 8 and 22 h, cells were analyzed using a plate reader with excitation and emission wavelengths of 485 and 530 nm, respectively. All treatments were performed in triplicate for each of three experiments.

2.4. Superoxide generation.

Superoxide generation was measured by MitoSOX^{TM} Red (Invitrogen, CA, USA). The cells were centrifuged and resuspended in fresh media at a concentration of 10^6 cells/mL and then washed in Hank's Balanced Salt Solution (HBSS), which was followed by the addition of 2.5 μM MitoSOX^{TM} Red and finally incubated for 30 minutes in a dark, humidified incubator at 37°C with 5% CO_2 to allow for uptake. Cells were subsequently washed again with HBSS to remove extracellular MitoSOX^{TM} Red, after which fresh media was added. Cells were then seeded in 96-well plates at 10^5 cells per well. NPs suspended in tissue culture media were then added for a final concentration of 10–100 μg/mL. Subsequently, cells with NPs were co-exposed with UVA (6.7 J/cm^2). After incubation time points of 1, 4, 8 and 22 h,

cells were fixed (in -20°C ethanol) and analyzed using flow cytometry (FACS Canto II, Becton, Dickinson and Co., Franklin Lakes, NJ, USA). All treatments were performed in triplicate for each of two experiments.

2.5. Statistics.

Data are presented as mean ± standard error of mean (SEM) and was analysed using two-way ANOVA and Bonferroni post hoc test (Prism 5.0, GraphPad Software, La Jolla, CA, USA), with a p value < 0.05 considered significant.

3. Results and discussion

3.1. Cytotoxicity of sunscreen NPs

The UVA component of sunlight's UV spectrum is 95%, with the remaining 5% being the UVB component that causes erythema of the skin. The UVA dose used in this study was the UVA component of sunlight corresponding to 1.67-fold of the Minimal Erythemal Dose (MED) (6.7 J/cm^2)[23], which is equivalent to the UVA component of approximately 30 min of noonday summer sun in Sydney, Australia, at 33.86°S latitude. The viability of THP-1 monocytes 24 h after exposure to UVA dose was unchanged and was 103.5 ± 1.7%, compared to the viability in untreated cells of 100.0 ± 2.2% (n=3 experiments). Whilst NPs themselves demonstrated cytotoxicity at >10 μg/mL[20], the cell viability after 24 h was not significantly altered with

co-exposure to both UVA and sunscreen NPs [Fig. 1], which indicates that the UVA dose used in this study is not directly cytotoxic.

3.2. Peroxide generation.

In measuring intracellular peroxide generation, we employed the ROS fluorophore DCFDA, which is sensitive to all forms of peroxide, including hydrogen peroxide.[24] We observed that UVA exposure induced high levels of intracellular peroxide, i.e. at 1 h the peroxide levels were 7-fold higher than that of sham-irradiated control [Fig. 2]. UVA-induced peroxide generation steadily increased over time (though not statistically significant, $p=0.18$) and by 22 h it was 8.5-fold higher than that observed in the sham-irradiated controls at 1 h [Fig. 2A]. This fixed-time point control comparator was necessary as we also observed that when comparing the peroxide generation at each time point to its respective sham control at that same time point, there was an apparent decrease in relative UVA-induced peroxide generation over time [Fig. 2B]. This experimental artefact was due to changes in the test to control ratios that were a product of both treatment and control peroxide levels increasing over time, most likely as a function of normal cellular metabolism.[25] This is illustrated by the observation that the peroxide generated by the sham control increased by an amount very similar to the UVA-treated control [Fig. 2A]. Thus, when expressed as a ratio of its respective sham control, the 24 h value is approximately half that of the value obtained from the 1 h time point [Fig. 2B], which may be a significant confounder in

the interpretation of time course measurements using DCFDA, or indeed any measurement of this fluorophore at a single time point.

In this study, we also employed hydrogen peroxide (H_2O_2) at 1 mM as a positive control. This concentration of H_2O_2 was chosen to generate the same level of peroxide ROS in THP-1 monocytes as the experimental UVA dose (6.7 J/cm^2) [Supplementary material Fig. S1]. The kinetic profile of peroxide generation over 22 h for 1 mM H_2O_2 and that induced by 6.7 J cm^{-2} UVA was also very similar. In Fig. S1A, the time course of the peroxide generation in H_2O_2-treated cells increased from 7-fold at 1 h to 8.5-fold at 22 compared to the 1 h sham control. Again, this increase in cellular peroxide is likely to be from normal cellular metabolism and shows that these DCFDA artefacts are consistent across different experimental systems for this cell type.

In order to compare UV-induced peroxide production to sunscreen NP-generated peroxide, cells were exposed to NPs both with and without UVA co-exposure. Overall, the co-exposure of cells to ZnO NPs and UVA showed a dose-dependent decrease in intracellular peroxide generation [Fig. 3]. At low and intermediate doses of the pristine ZnO 30 nm ("ZnO 30") or ZnO 200 nm ("ZnO 200") particulates that did not directly alter cell viability (i.e. 10 and 50 μg/mL) [Fig. 1], the intracellular peroxide levels were not significantly altered by co-exposure with UVA. At the highest dose (100 μg/mL) these particulates decreased intracellular peroxide levels, but also reduced cell viability.

The ZnO 30nm, modified with Orotan surfactant (denoted as "sZnO 30"), was seen to be the most effective particulate, by significantly reducing the peroxide

generation in UVA co-exposed monocytes at the intermediate dose (50 μg/mL) [Fig. 3]. At the highest dose, the surfactant-dispersed ZnO NPs further decreased peroxide levels, but also markedly reduced cell viability. Therefore, as the lowest dose of sZnO 30 NPs did not alter cell viability, this slight reduction in peroxide appeared to be mainly attributable to attenuation of UV by the particles, even in their dispersed state. In order to verify this, we measured the UV-vis spectra of the three particulates, which confirmed a much higher absorbance for sZnO 30 than for ZnO 30 in the UVA spectral wavelengths [Supplementary material Fig. S2]. The difference between the absorbance of sZnO 30 and ZnO 30 is presumably a reflection of the degree of agglomeration and consequent increased diffuse light scattering observed with the surfactant-dispersed sZnO 30. We also found no significant differences in UVA absorbance for ZnO 200 and ZnO 30, which would explain why their peroxide generation profile was very similar [Fig. 3]. As expected, this UVA attenuation also increased with dose, which may account for the observed decreases in peroxide generation in THP-1 monocytes with increasing NP dose.

The concentration of ZnO NPs required in this system to generate detectable levels of ROS was close to the concentrations required to induce cytotoxicity. As the three ZnO particulates displayed different cytotoxicity profiles, the respective contributions of reduced viable cell number versus UVA attenuation towards the decreased peroxide generation varied between these particulates. Re-plotting Fig. 3 as a ratio of the respective UVA control for each time point (as opposed to the 1 h UVA

control) resulted in different profiles in which peroxide generation did not increase over time [Supplementary material Fig. S3] – as was discussed previously for the UVA and H_2O_2 positive control data.

Two forms of TiO_2 were examined, one of primarily anatase crystalline structure and the other being primarily rutile, with similar particle sizes but different shapes. Titania NPs, unlike ZnO, did not cause cytotoxicity in UVA-exposed cells at concentrations less than 1 mg/mL [Supplementary material Fig. S4]. The observed peroxide production profile in the TiO_2-UVA co-exposure system was different between the crystalline forms, with anatase TiO_2 NPs behaving substantially different from both rutile and ZnO NPs [Fig. 4]. For anatase TiO_2 NPs, the peroxide levels increased with increasing concentration [Fig. 4]. In contrast, rutile TiO_2 behaved similarly to ZnO, with peroxide levels decreasing with increasing concentrations. Consequently at the highest dose of 100 μg/mL TiO_2, the peroxide generated by cells exposed to anatase in the presence of UVA was twice that seen with rutile and UVA co-exposure [Supplementary material Fig. S5]. As the anatase phase of TiO_2 is known to be more photocatalytic than rutile[8], this result was not unexpected. Interestingly, the rutile material was not entirely pure (as is typical of TiO_2), yet clearly the small amount of anatase present was not sufficient to induce biologically relevant levels of peroxide. This critical threshold for anatase levels, above which ROS production is no longer reduced, is obviously very important in determining the most desirable form of TiO_2 NPs for use in sunscreens. However, it needs to be noted that the increased

generation of ROS by co-exposure to anatase TiO_2 and UVA irradiation was still insufficient to reduce cell viability, until extremely high concentrations were used (1 mg/mL) [Supplementary material Fig. S4].

In the absence of UVA [Supplementary material Fig. S6], we observed that ZnO and TiO_2 alone generated much less peroxide than with UVA exposure alone [Fig. 2]. The peroxide generated by UVA alone in this study was 6-7 fold higher than that produced by all of the particulates. Furthermore, co-exposure to UVA and ZnO or rutile TiO_2 NPs results in less peroxide generation than from UVA alone. Taken together, we can conclude that the levels of peroxide induced by ZnO and rutile TiO_2 NPs, when concentrated into immune cells, are not a significant concern. High anatase TiO_2 containing materials are an exception, as peroxide generation was enhanced in UVA and anatase NP co-exposure compared to UVA alone. Even in this case, recent skin penetration studies suggest that intact sunscreen NPs do not penetrate beyond the stratum corneum of healthy skin[26–28], meaning that the exposure of viable cells to NPs is likely to be negligible, especially as the effect of peroxides formed at or near the skin surface will be diffusion limited.

3.3. Superoxide generation

UVA-irradiated cells also produced high levels of mitochondrial superoxide when compared to negative controls [Fig. 5]. However, these increased levels of superoxide were not as high as peroxide levels produced under UVA, as superoxide levels were

3.3 fold higher at the 1 h time point compared to the 7-fold higher peroxide generation. This suggests that cytoplasmic peroxide is more inducible by UVA than mitochondrial superoxide. Furthermore, mitochondrial superoxide levels did not change significantly over time, in contrast to the steady increase observed in intracellular peroxide levels. This suggests that normal cellular metabolism generates superoxide quite slowly, or that superoxide accumulation is tightly controlled in the mitochondria by protective antioxidant pathways.[29]

In order to investigate the effect of UVA and NP co-exposure, we compared the mitochondrial superoxide generation after exposure to NPs at either equivalent cytotoxicities (EC50) for ZnO or at 100 µg/mL for TiO_2 NPs, with and without UVA irradiation. At the 1 h time point, with the exception of anatase TiO_2, the other NPs did not alter superoxide generation [Fig. 6]. This again reinforces that anatase TiO_2 generates ROS (both cytoplasmic peroxide and mitochondrial superoxide) under UVA, and is therefore not an ideal UV filtering component for use in sunscreen formulations.

In the absence of UVA [Supplementary material Fig. S7], we observed that ZnO and TiO_2 NPs alone generated much less mitochondrial superoxide than with UVA exposure alone. The mitochondrial superoxide generated by UVA alone in this study was twice that produced by all of the particulates.

The kinetics for mitochondrial superoxide generation in cells with UVA and particulate co-exposure was also different to that for peroxide generation [Fig. 6]. In TiO_2-exposed cells, superoxide levels continued to gradually decrease over time after the initial rapid decline for anatase-exposed cells, whereas both ZnO 30 and sZnO 30 marginally increased mitochondrial superoxide levels over the same period. A possible explanation for these differences is that while cellular metabolism efficiently reduces mitochondrial superoxide (as illustrated by the decreased TiO_2 signal), ZnO itself appears to induce further mitochondrial superoxide. In our previous studies, we have shown a strong relationship between intracellular zinc ion levels (elevated by dissolution of endocytosed ZnO NPs) and mitochondrial superoxide generation.[20] Therefore these cells must cope with combined superoxide generation from two sources (UVA and zinc ion-mediated), leading to a net positive increase over the 22 h period. This marginal increase in ZnO NP-induced superoxide production strongly correlates with "soluble" or readily bioavailable zinc from the NPs and appears to be a more significant influence on the mitochondrial superoxide system over this time than UVA exposure.

Clearly, the least reactive test material in this system was rutile TiO_2, where exposed cells produced less cytoplasmic peroxide and mitochondrial superoxide, and showed no significant loss in viability. Whilst ZnO NPs appear to be more bioactive than rutile, they have several preferred characteristics for use in sunscreens. These include: the larger ZnO particle size further reduces skin penetration potential[18,27]; its

solubility in sweat and the acidic conditions within endosomes reduce its potential for persistence on skin and in the body (compared to the very insoluble TiO_2); that zinc as an essential metal ion with tightly-regulated mammalian homeostatic mechanisms (while TiO_2 is not biologically essential); and the reactivity of ZnO in the environment[30], reducing its potential for environmental biopersistence and ecotoxicity.

4. Conclusions

In this study, we investigated intracellular peroxide and mitochondrial superoxide generation of sunscreen NP-exposed THP-1 monocytes in the presence and absence of UVA. These cells, as accumulators of particulates in body fluids and tissues, would be expected to have higher levels of NP exposure and thus should be the primary focus for ROS induced by UVA and NP co-exposure in the skin. We demonstrated that, with the exception of anatase TiO_2, ROS generation in these human immune cells from sunscreen NP and UVA co-exposure is less than or equal to cellular ROS produced by UVA alone. The implications of this observation are that, whilst chemically it may be possible to demonstrate significant ROS activity in these materials over extended periods of UV exposure (such as with painted metal surfaces), at a biological level the quantity of ROS these NPs produce even in the presence of UV is insignificant compared with normal environmental stumuli (i.e. UV light itself).

For sunscreen formulations, photocatalytic ROS generation induced by ZnO NPs and TiO_2 NPs of low anatase content appear to be of very low toxicological concern.

Acknowledgements

This project was supported by National Health and Medical Research Council (NHMRC, Australia) project grant #616621, Advanced Manufacturing Cooperative Research Centre (AMCRC), The Victorian Centre for Advanced Materials Manufacturing Ltd (VCAMM). Cenchao Shen was the recipient of Postgraduate Scholarships from the NHMRC and AMCRC. We thank Micronisers Australasia Pty Ltd. for the supply of samples and Baxter Laboratories Pty Ltd for helpful discussions.

References

1. K. Scharffetter-Kochanek, M. Wlaschek, P. Brenneisen, M. Schauen, R. Blaudschun and J. Wenk, UV-induced reactive oxygen species in photocarcinogenesis and photoaging, *Biol. Chem.,* 1997, **378**, 1247-1257.
2. M. Ichihashi, M. Ueda, A. Budiyanto, T. Bito, M. Oka, M. Fukunaga, K. Tsuru and T. Horikawa, UV-induced skin damage, *Toxicology,* 2003, **189**, 21-39.
3. K. M. Hanson, E. Gratton and C. J. Bardeen, Sunscreen enhancement of UV-induced reactive oxygen species in the skin, *Free Radic. Biol. Med.,* 2006, **41**, 1205-1212.
4. C. Paris, V. Lhiaubet-Vallet, O. Jimenez, C. Trullas and M. A. Miranda, A blocked diketo form of avobenzone: Photostability, photosensitizing properties and triplet quenching by a triazine-derived UVB-filter, *Photochem. Photobiol.,* 2009, **85**, 178-184.
5. R. Roy, V. Parashar, L. K. Chauhan, R. Shanker, M. Das, A. Tripathi and P.D. Dwivedi, Mechanism of uptake of ZnO nanoparticles and inflammatory responses in macrophages require PI3K mediated MAPKs signalling. *Toxicol. In Vitro,* 2014, **28**, 457–67.
6. D. Sahu, G. M. Kannan and R. Vijayaraghavan, Size-dependent effect of zinc oxide on toxicity and inflammatory potential of human monocytes, *J. Toxicol. Environ. Health A*. 2014, **77**, 177–91.

7. K. N. Yu, T. J. Yoon, A. Minai-Tehrani, J. E. Kim, S. J. Park, M. S. Jeong, S. W. Ha, J. K. Lee, J. S. Kim and M. H. Cho, Zinc oxide nanoparticle induced autophagic cell death and mitochondrial damage via reactive oxygen species generation, *Toxicol. In Vitro,* 2013, **27**, 1187–95.

8. P. J. Barker and A. Branch, The interaction of modern sunscreen formulations with surface coatings, *Prog. Org. Coat.,* 2008, **62**, 313-320.

9. T. Xia, M. Kovochich, M. Liong, L. Madler, B. Gilbert, H. Shi, J. I. Yeh, J. I. Zink and A. E. Nel, Comparison of the mechanism of toxicity of zinc oxide and cerium oxide nanoparticles based on dissolution and oxidative stress properties, *ACS Nano,* 2008, **2**, 2121-2134.

10. T. Xia, M. Kovochich, J. Brant, M. Hotze, J. Sempf, T. Oberley, C. Sioutas, J. I. Yeh, M. R. Wiesner and A.E. Nel, Comparison of the abilities of ambient and manufactured nanoparticles to induce cellular toxicity according to an oxidative stress paradigm, *Nano Lett.,* 2006, **6**, 1794-1807.

11. L. K. Braydich-Stolle, N. M. Schaeublin, R. C. Murdock, J. Jiang, P. Biswas, J. J. Schlager and S. M. Hussain, Crystal structure mediates mode of cell death in TiO_2 nanotoxicity, *J. Nanopart. Res.,* 2009, **11**, 1361-1374.

12. W. S. Lin, Y. Xu, C. C. Huang, Y. F. Ma, K. B. Shannon, D. R. Chen and Y. W. Huang, Toxicity of nano- and micro-sized ZnO particles in human lung epithelial cells, *J. Nanopart. Res.,* 2009, **11**, 25-39.

13. A. Nel, T. Xia, L. Madler and N. Li, Toxic potential of materials at the nanolevel, *Science,* 2006, **311**, 622-627.

14. C. Hanley, A. Thurber, C. Hanna, A. Punnoose, J. H. Zhang and D. G. Wingett, The influences of cell type and ZnO nanoparticle size on immune cell cytotoxicity and cytokine induction, *Nanoscale Res. Lett.,* 2009, **4**, 1409-1420.

15. N. A. Monteiro-Riviere, K. Wiench, R. Landsiedel, S. Schulte, A. O. Inman and J. E. Riviere, Safety evaluation of sunscreen formulations containing titanium dioxide and zinc oxide nanoparticles in UVB sunburned skin: an *in vitro* and *in vivo* study, *Toxicol. Sci.* 2011, **123**, 264–80.

16. A. Jebali and B. Kazemi, Triglyceride-coated nanoparticles: skin toxicity and effect of UV/IR irradiation on them, *Toxicol. In Vitro,* 2013, **27,** 1847–54.

17. G. M. Halliday, S. N. Byrne and D. L. Damian, Ultraviolet A radiation: its role in immunosuppression and carcinogenesis, *Semin. Cutan. Med. Surg.,* 2011, **30**, 214-221.

18. B. Gulson, M. McCall, M. Korsch, L. Gomez, P. Casey, Y. Oytam, A. Taylor, M. McCulloch, J. Trotter, L. Kinsley and G. Greenoak, Small amounts of zinc from zinc oxide particles in sunscreens applied outdoors are absorbed through human skin, *Toxicol. Sci.,* 2010, **118**, 140-149.

19. B. N. Feltis, S. J. O'Keefe, A. J. Harford, T. J. Piva, T. W. Turney and P. F. A. Wright, Independent cytotoxic and inflammatory responses to zinc oxide

nanoparticles in human monocytes and macrophages, *Nanotoxicology,* 2012, **6**, 757-765.

20. C. Shen, S. A. James, M. D. de Jonge, T. W. Turney, P. F. Wright and B. N. Feltis, Relating cytotoxicity, zinc ions, and reactive oxygen in ZnO nanoparticle-exposed human immune cells, *Toxicol. Sci.,* 2013, **136**, 120-130.
21. T. W. Turney, M. B. Duriska, A. Elbaz, S. J. O'Keefe, T. J. Piva, P. F. A. Wright and B. N. Feltis, Formation of zinc-containing nanoparticles from Zn^{2+} ions in cell culture media: Implications for the nanotoxicology of ZnO, *Chem. Res. Toxicol.*, 2012, **25**, 2057–2066
22. C. Singh, S. Friedrichs, M. Levin, R. Birkedal, K. A. Jensen, G. Pojana, W. Wohlleben, S. Schulte, K. Wiench, T. Turney, O. Koulaeva, D. Marshall, K. Hund-Rinke, W. Kördel, E. Van Doren, P-J. De Temmerman, M. Abi Daoud Francisco, J. Mast, N. Gibson, R. Koeber, T. Linsinger and C. L. Klein, NM-Series of representative manufactured nanomaterials – zinc oxide NM-110, NM-111, NM-112, NM-113 characterisation and test item preparation, EUR 25066 EN, European Commission Joint Research Centre, Institute for Reference Materials and Measurements, Publications Office of the European Union, Luxembourg, 2011, ISBN 978-92-79-22215-3.
23. J. M. Kuchel, R. S. Barnetson and G. M. Halliday, Ultraviolet A augments solar-simulated ultraviolet radiation-induced local suppression of recall responses in humans, *J. Invest. Dermatol.,* 2002, **118**, 1032-1037.

24. B. Halliwell and M. Whiteman, Measuring reactive species and oxidative damage *in vivo* and in cell culture: how should you do it and what do the results mean? *Br. J. Pharmacol. Discipline Pharmacology,* 2004, **142**, 231-255.

25. B. Poljsak, Z. Gazdag, S. Jenko-Brinovec, S. Fujs, M. Pesti, J. Belagyi, S. Plesnicar and P. Raspor, Pro-oxidative vs antioxidative properties of ascorbic acid in chromium(VI)-induced damage: an *in vivo* and *in vitro* approach, *J. Appl. Toxicol.,* 2005, **25**, 535-548.

26. A. Elder, S. Vidyasagar and L. DeLouise, Physicochemical factors that affect metal and metal oxide nanoparticle passage across epithelial barriers, *Wiley Interdiscip. Rev. Nanomed. Nanobiotechnol.,* 2009, **1**, 434-450.

27. A. V. Zvyagin, X. Zhao, A. Gierden, W. Sanchez, J.A. Ross and M. S. Roberts, Imaging of zinc oxide nanoparticle penetration in human skin *in vitro* and *in vivo*, *J. Biomed. Opt.,* 2008, **13**, 064031.

28. N. Sadrieh, A. M. Wokovich, N. V. Gopee, J. W. Zheng, D. Haines, D. Parmiter, P. H. Siitonen, C. R. Cozart, A. K. Patri, S. E. McNeil, P. C. Howard, W. H. Doub and L. F. Buhse, Lack of significant dermal penetration of titanium dioxide from sunscreen formulations containing nano- and submicron-size TiO_2 particles, *Toxicol. Sci.,* 2010, **115**, 156-166.

29. S. Miriyala, A. K. Holley and D. K. St Clair, Mitochondrial superoxide dismutase – signals of distinction, *Anticancer Agents Med. Chem.,* 2011, **11**, 181-190.

30. E. Lombi, E. Donner, E. Tavakkoli, T. W. Turney, R. Naidu, B. W. Miller and K. G. Scheckel, Fate of zinc oxide nanoparticles during anaerobic digestion of wastewater and post-treatment processing of sewage sludge, *Environ. Sci. Technol.,* 2012, **46**, 9089-9096.

Figure Legends

Fig. 1 Cell viability of human THP-1 monocytes after 24 h exposure to sunscreen NPs, following initial co-exposure to 6.7 J/cm^2 UVA (mean ± SEM, n=3 experiments). All concentrations at or below the horizontal line were highly significantly different from control cells receiving UVA irradiation alone ($p < 0.001$).

Fig. 2 Generation of intracellular peroxide by THP-1 monocytes over the 22 h time course after initial exposure to 6.7 J/cm^2 UVA; represented as a ratio of the sham control at 1 h (A), and as a ratio of the respective sham control for each time point (B) (mean ± SEM, n=3 experiments in triplicate).

Fig. 3 Generation of intracellular peroxide by THP-1 monocytes over the 22 h time course after exposure to ZnO 30 NPs or ZnO 200 bulk particles at 10 µg/mL (A), 50 µg/mL (B), and 100 µg/mL (C), following initial co-exposure to 6.7 J/cm^2 UVA; represented as a ratio of the sham control at 1 h (mean ± SEM, n=3 experiments in triplicate). Time points marked with stars were significantly different from control cells receiving UVA irradiation alone (* $p < 0.05$, ** $p < 0.01$, *** $p < 0.001$).

Fig. 4 Generation of intracellular peroxide by THP-1 monocytes after 1 h (A), 4 h (B), 8 h (C) and 22 h (D) exposure to ZnO or TiO_2 NPs, following initial co-exposure to 6.7 J/cm^2 UVA; represented as a ratio of the sham control at 1 h (mean ± SEM, n=3 experiments in triplicate). Concentrations marked with stars were significantly different from control cells receiving UVA irradiation alone (* $p < 0.05$, ** $p < 0.01$, *** $p < 0.001$).

Fig. 5 Generation of mitochondrial superoxide by THP-1 monocytes over the 22 h time course, following initial exposure to 6.7 J/cm^2 UVA; represented as a ratio of the sham control at 1 h (A), and as a ratio of the respective sham control for each time point (B) (mean ± SEM, n=2 experiments in triplicate).

Fig. 6 Generation of mitochondrial superoxide by THP-1 monocytes over 22 h exposure to ZnO or TiO_2 NPs, following initial co-exposure to 6.7 J/cm^2 UVA; represented as a ratio of the sham control at 1 h (mean ± SEM, n=2 experiments in triplicate). Time points marked with stars were significantly different from control cells receiving UVA irradiation alone (* $p < 0.05$).

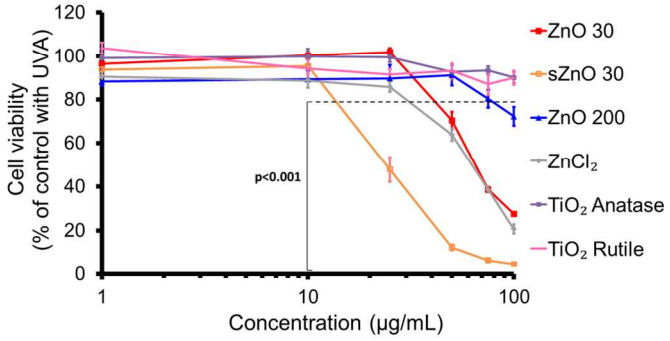

140x59mm (600 x 600 DPI)

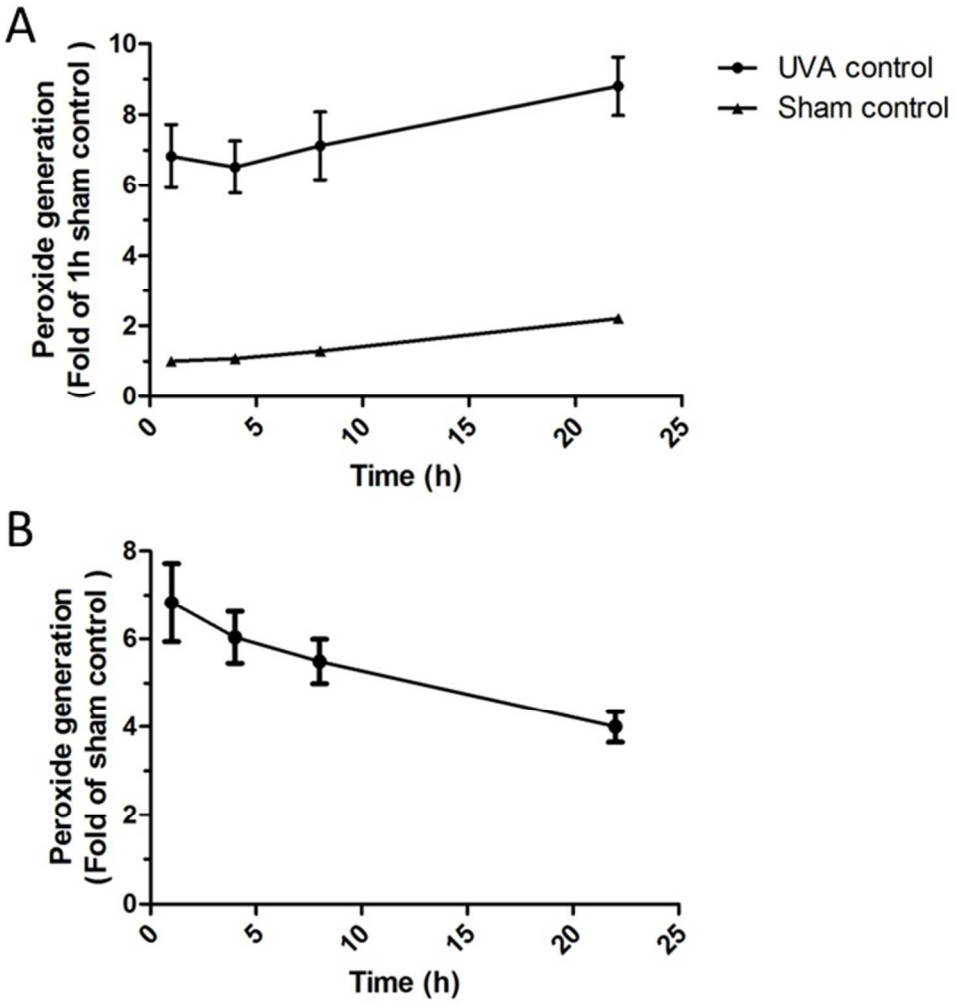

152x160mm (600 x 600 DPI)

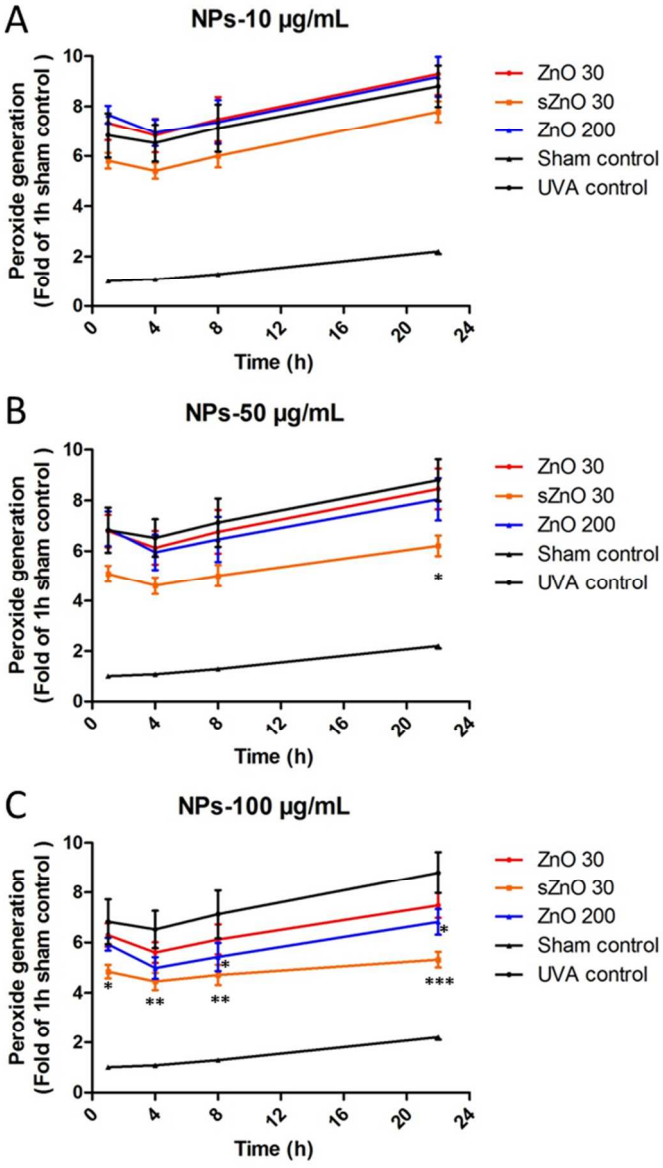

225x387mm (600 x 600 DPI)

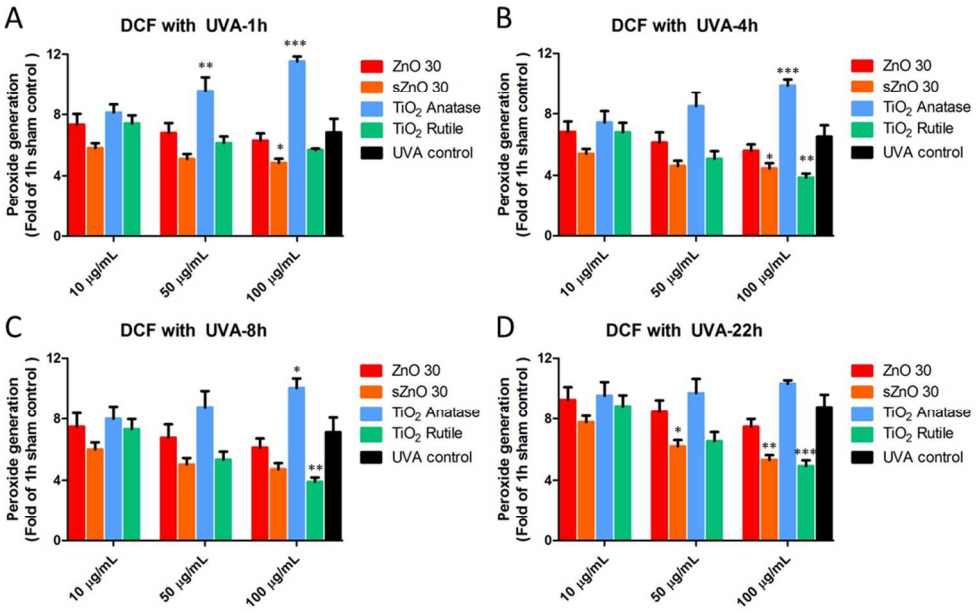

154x97mm (600 x 600 DPI)

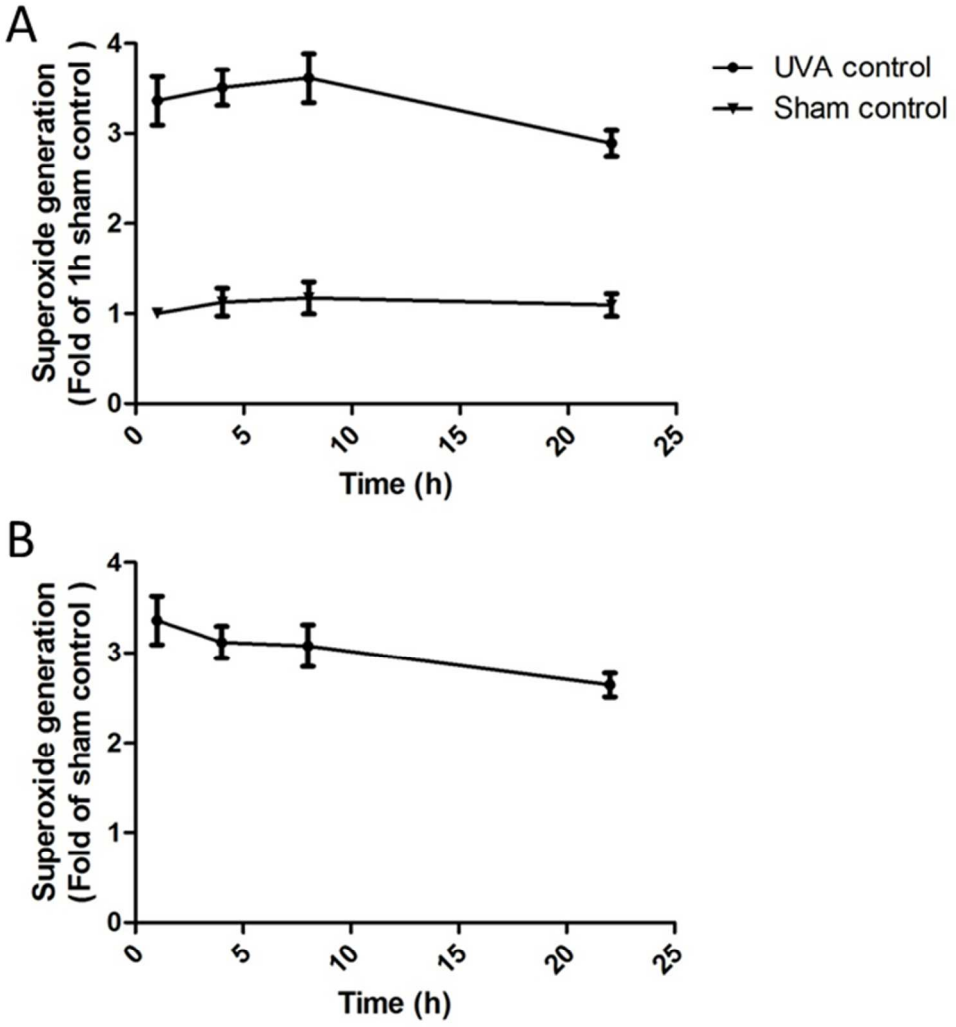

153x164mm (600 x 600 DPI)

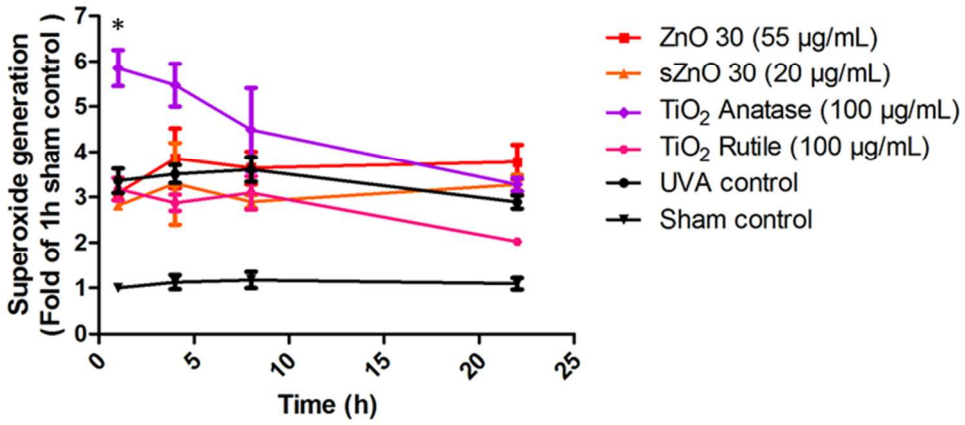

76x35mm (600 x 600 DPI)

Manuscript ID PP-ART-12-2013-050428

Graphical Abstract (colour picture has been cropped from Figure 4)

"Comparison of UVA-induced ROS and sunscreen nanoparticle-generated ROS in human immune cells"

Cenchao Shen, Terence W. Turney, Terrence J. Piva, Bryce N. Feltis & Paul F.A. Wright

Graphical Abstract text:

Generation of reactive oxygen species in human immune cells co-exposed to UVA and ZnO or rutile TiO_2 nanoparticles is not greater than that produced in the cells by UVA alone.